HARMONIA
International network for harmonization of atmospheric aerosol retrievals from ground based photometers

HARMONIA CA21119

Deliverable 1.4

Spectral AOD and AOD in the UV

Authors	Angelos Karanikolas[1,3], Lionel Doppler[2], Peter Hrabčák[4], Katerina Anyfanti[5]
Date	23 October 2026

[1]Radiation Center, Physikalisch-Meteorologisches Observatorium Davos / World Radiation Center (PMOD/WRC), Davos, Switzerland

[2]Meteorologisches Observatorium Lindenberg - Richard-Aßmann-Observatorium, Deutscher Wetterdienst (MOL-RAO, DWD), Lindenberg (Tauche), Germany

[3]Institute for Particle Physics and Astrophysics, ETH Zurich, Zurich, Switzerland

[4]Aerological and Solar Radiation Center, Slovak Hydrometeorological Institute, Gánovce, Slovakia

[5]Research Centre for Atmospheric Physics and Climatology, Academy of Athens, Athens, Greece.

cost EUROPEAN COOPERATION IN SCIENCE & TECHNOLOGY

Funded by the European Union

Contents

1. Introduction 2
2. Methods 5
2.1 General methods for spectral AOD retrieval 5
2.2 Specificities of AOD retrieval in the UV 6
2.3 Specificities of AOD retrieval in the IR 7
3. Former studies and publications 8
3.1 AOD retrieval in the UV 8
3.1.1 UV AOD Retrievals with Brewers 8
3.1.2 Validation of AOD from UV spectroradiometers 15
3.2 Spectral AOD retrievals in VIS and IR 16
3.3 AOD retrieval from MAX-DOAS instruments 20
4. Spectral AOD with high spectral range and resolution 21
4.1 Methodology 21
4.2 Results and discussion 23
5. Summary 30
References 32
List of figures 42
Appendix 43
Acknowledgements 45

1. Introduction

Aerosols are a highly heterogeneous atmospheric component with various effects on Earth. They interact with solar radiation and clouds, affecting climate and weather. They also impact air quality, affect plant development and aviation. Aerosol optical depth (AOD) describes the overall effect of aerosols on radiation extinction and therefore is the most comprehensive variable for climate studies (WMO, 2003). It is defined for each wavelength as part of the exponent in the Beer-Lambert-Bouguer law:

$$I = I_o e^{-m\tau} \quad (1)$$

where I is the direct solar irradiance on the ground at a particular wavelength, I_o the direct solar irradiance at the top of the atmosphere at the same wavelength, m the optical air mass coefficient and τ the total optical depth of the atmosphere. τ is the sum of all individual optical depths of each atmospheric component (gases and aerosols).

In a given time and location AOD varies with the wavelength of radiation, typically increasing for shorter wavelengths. The most typical approximation for the AOD spectral dependence is the Ångström law:

$$\tau = \beta\lambda^{-\alpha} \quad (2)$$

where τ is the AOD, β is the turbidity coefficient, λ the wavelength and α the Ångström exponent (AE). The turbidity coefficient is related to the aerosol load and AE to the size of aerosols.

The Ångström law describes the behaviour of AOD within the typical conditions and measured wavelengths, but there can be cases of significant deviations as we will show later.

The conventional instruments that measure AOD are filter radiometers, which measure irradiance at specific wavelengths with low gas absorption. Certain filter radiometers (named also Sun photometers) are used by international networks such as Aerosol Robotic Network (AERONET), Global Atmosphere Watch - Precision Filter Radiometer (GAW-PFR) or SKYNET (Doppler et al., 2023-Deliverable 1.1;

Kazadzis et al., 2018). AERONET uses the CIMEL CE318-T - Sun and Sky Photometer (CIMEL), GAW-PFR the Precision Filter Radiometer (PFR), while SKYNET as primary instrument the PREDE-POM sun sky radiometer (POM). Some of their wavelengths are common or directly comparable. Nominally 500 nm is a common channel for all 3 networks, while 870 nm is common to AERONET and SKYNET, with GAW-PFR measuring at 862 nm. 1020 nm is another common channel between AERONET and SKYNET, while the availability of 340 nm depends on the version of the SKYNET instrument. This makes it easier to assess the homogeneity between the networks, which is the subject of deliverables 1.1 and 1.3 (Doppler et al., 2023; Doppler et al., 2026). However, it also means that regular AOD observations are limited to a small set of wavelengths over a limited spectral range (typically 340-1020 nm or even 368-862 nm). Certain AERONET instruments provide one additional channel at 1640 nm, where AOD is lower, gas absorption higher and the AOD observations more limited since it is not included in the other 2 networks. Similarly, the extended version of SKYNET instruments (POM-02) includes the 1627 and 2200 nm channels, with the main goal of studying cloud properties (Wang et al., 2014). As a result, studying the behaviour of AOD beyond the typical wavelengths requires modelling or extrapolation of observed AOD with a smooth function, either the Ångström law or some fitting method (such as polynomial). Such smooth functions may typically perform well between the wavelengths measured by filter radiometers (Kazadzis et al., 2023) but the behaviour at different spectral regions such as further in the ultraviolet (UV) or infrared (IR) could be different, while certain unusual aerosol cases may show larger deviations in any spectral band.

Aside from filter radiometers there are other instruments measuring direct solar irradiance spectrally, such as spectroradiometers. Spectroradiometers measure irradiance at much higher spectral resolution with possible intervals of measurements 0.5 nm or less. This may result in more than 1000 wavelengths within a spectral range for which a conventional filter radiometer may measure at only at 4-8 wavelengths, and they can also cover a longer spectral range.

Retrieving AOD in the UV is a particularly interesting case. UV is a biologically active spectral region both positively (vitamin D production in humans) and negatively (DNA damage) (Häder et al., 2005; Grant, 2007; Bais et al., 2019). UV is a regularly measured spectral region that became particularly relevant due to ozone depletion

(Molina and Rowland, 1974; WMO, 2022) with instruments such as Dobson and Brewer spectrophotometers providing long time series (Staehelin et al., 2018; Garane et al., 2024). Filter radiometers typically provide AOD at 340, 368 or 380 nm, so in the UV-A region close to the visible spectrum where ozone absorption is minimal or even negligible with the exception of a particular version of PFR different than the standard one (Carlund et al., 2017). Spectroradiometers on the other hand with high spectral resolution can cover a wider wavelength range in the UV, including wavelengths where ozone absorption is either stronger or weaker. Yet, this is one of the challenges for AOD retrieval in that region, as we will show in the following sections.

The IR became more relevant due to global warming since it allows us to measure greenhouse gases. This is part of the challenge in retrieving AOD due to the large number of spectral lines and bands with strong absorption by water vapour (H_2O) or other gases such as carbon dioxide (CO_2), which significantly limit the spectral regions available for AOD retrievals. Yet, the IR is useful for the characterisation of larger particles (more in Section 4), and in certain regions the gas absorptions can be relatively weak, even beyond 1020 nm.

In this deliverable, we aim to provide an overview of studies related to AOD retrieval from spectroradiometers, examples of retrievals beyond the conventional channels and discussion on the behaviour of AOD, the status and the difficulties of such observations.

2. Methods

2.1 General methods for spectral AOD retrieval

Details of the methodology of the AOD retrieval are in Deliverables 1.2, 1.3 and 2.3 (Doppler et al., 2024; Doppler et al., 2026; Kazadzis et al., 2024) of the present COST action. Therefore, here we provide a brief summary. To retrieve AOD, we typically apply Eq. 1 to solar radiation measurements. Therefore, we require direct solar irradiance measurements under conditions with no clouds in front of the solar disc, at specific wavelengths for which we are able to calculate the gas absorption optical depth. We also need to know the position of the Sun, the irradiance the instrument would measure at the top of the atmosphere, and the optical depth of molecular scattering. The solar zenith angle (SZA) is usually available as a primary output from the software responsible for controlling the corresponding instruments and providing the 'raw' output, including the measured irradiance. Through adapted formulas, we can calculate the optical air mass of the atmosphere, aerosols and specific gases absorbing radiation at the wavelengths our instrument measures (Doppler et al., 2026-deliverable 1.3; Cuevas et al., 2019). The irradiance at the top of the atmosphere is known only for calibrated instruments. The main calibration method is the Langley plot (Shaw et al., 1973), which we can apply from the ground at high-altitude stations. Rayleigh (molecular) scattering optical depth can be calculated through the atmospheric pressure with different formulas (Doppler et al., 2026-deliverable 1.3; Cuevas et al., 2019). Gas absorption optical depth can be calculated from the absorption cross section and total column of each gas, which means we need to know which gases absorb radiation and their total columns at that particular time and location. Moreover, under strong gas absorption, any error in the total column measurements of the corresponding gas can result in a large error in AOD. Therefore, conventional instruments that measure AOD (filter radiometers) measure irradiance at carefully selected wavelengths for their minimal gas absorption from the atmosphere, which is mostly caused by regularly measured gases such as ozone (O_3), nitrogen dioxide (NO_2) and water vapour (H_2O).

On the other hand, because spectroradiometers measure irradiance at a much higher spectral resolution, they can provide us with the capability to retrieve AOD at

additional wavelengths (as long as the spectroradiometer is calibrated and as long as simultaneous measurements of the total columns of certain gases - which we can use for AOD correction - are available). Both filter radiometers and spectroradiometers can be calibrated by the Langley plot method (Shaw et al., 1973). They can also be calibrated in W/m^2 with lamps or lasers of known intensity (Kouremeti et al., 2022). In that case, the top-of-the-atmosphere radiation is available through satellite measurements. Then, AOD can be retrieved in the same way as described above.

2.2 Specificities of AOD retrieval in the UV

The UV spectral region is subject to a large number of studies. As mentioned, there are different instruments that measure UV radiation to retrieve trace gases (O_3, NO_2, SO_2), and some of them are suitable for AOD retrievals as well. Aside from the typical instruments and wavelengths mentioned in the introduction, there is a UV version of the Precision Filter Radiometer (UVPFR) providing AOD at 305, 311, 318 and 332 nm (Carlund et al., 2017). Another typical instrument for AOD in the UV is the Brewer spectrophotometer (Kerr et al., 1985). It typically measures from approximately 290 nm to 325 or 365.5 nm, depending on the version, with even newer versions extending to the visible spectrum. The spectral resolution is 0.5 nm. Although initially designed for O_3 and SO_2 measurements, there are currently long time series of high-resolution direct or even global irradiance.

One of the main challenges of AOD in the UV at shorter wavelengths than those measured by conventional filter radiometers is the correction of ozone absorption, particularly below 320 nm. Spectroradiometers that provide reliable ozone column measurements, such as the Brewers, are useful for this purpose. Using the same instrument for both ozone and AOD reduces the need for more instruments and the chance of mismatches between the ozone column used for AOD correction and the actual ozone column at the time of AOD measurement. However, Brewer spectrophotometers measure full direct spectra and ozone in separate modes. During direct or global irradiance scans, they measure each wavelength separately, and the scan takes some time to complete. The same applies to the reference spectroradiometers QASUME (Gröbner et al., 2023). On the other hand, instruments such as the UV-BiTech sensor (UV-BTS) (Zuber et al., 2018) and spectroradiometers suitable for the Multi-Axis Differential Optical Absorption Spectroscopy (MAX-DOAS)

technique (Hönninger et al., 2004), such as the Pandora spectrometer (Liu et al., 2024), are able to measure more frequently and provide coincident measurements of all wavelengths.

The methodology of AOD retrieval in the UV is similar to that described in Section 2.1, but it is even more important to correct ozone absorption properly. Therefore, the use of satellite retrievals or climatologies (a typical strategy of filter radiometer networks) can result in large errors. Also, NO_2 or even SO_2 absorption corrections may be important depending on the wavelength and the location, while conventional filter radiometer networks can neglect them when their stations are in low-pollution locations (GAW-PFR) or omit SO_2 and apply a correction based on climatologies, satellites (AERONET) or a fixed average for NO_2 (European SKYNET sub-network) without significant errors except extreme cases or wavelengths below 500 nm (Drosoglou et al., 2023; Masoom et al., 2024). Rayleigh scattering optical depth is also higher at shorter wavelengths. So, in the UV, the same relative error would result in a larger absolute AOD error.

2.3 Specificities of AOD retrieval in the IR

The IR spectral region is less studied than the UV in terms of solar radiation measurements and AOD retrievals, with more limited observations outside the main Sun photometric networks. The main challenge in the IR is that the total columns of greenhouse gases are not measured to the same extent as ozone. AERONET provides a total column of water vapour, while CO_2, methane (CH_4) and nitrous oxide (N_2O) are measured in situ as concentrations (Andrews et al., 2014; Komhyr et al., 1989) or by Fourier transform infrared spectroscopy (FTIR) as columns (Pathakoti et al., 2024), but only at a more limited number of locations. These locations often do not coincide with stations using instruments for AOD retrieval, making it challenging to correct those absorptions accurately. In Section 4, we provide an example of AOD retrievals under this challenge.

3. Former studies and publications

In this section, we perform a literature review of AOD retrievals from spectroradiometers. A prominent study including various spectroradiometers measuring from the UV to the near-IR is Gröbner et al. (2023). This study describes results from an intercomparison campaign in Izaña, Tenerife, with co-located instruments, including filter radiometers from AERONET and GAW-PFR and several spectroradiometers (QASUME, QASUME-IR, Precision Spectroradiometer or PSR, BTS) with various spectral ranges. It includes a comparison of top-of-the-atmosphere irradiance extrapolated from the spectroradiometers with a hybrid satellite-modelling product, showing 1% agreement for wavelengths unaffected by strong gas absorptions. It also shows the total optical depth in the range 300–2100 nm and, finally, AOD retrievals from all instruments at selected wavelengths or bands. All four spectroradiometers showed average AOD differences below 0.01 when compared to the reference filter radiometer at their common channels, showing very good potential for AOD retrievals with such instruments.

Below, we separate the overview into subsections related to the spectral region and type of study.

3.1 AOD retrieval in the UV

As mentioned in Section 2.2, AOD in the UV outside the conventional filter radiometers is mostly retrieved by Brewer spectrophotometers. Below, we provide an overview of such studies, and in another subsection, we include other instruments.

3.1.1 UV AOD Retrievals with Brewers

Brewers are quite old instruments, used since 70s for UV radiation and ozone monitoring. Savastiouk (1995) provided an algorithm that could be used to retrieve AOD from Brewer spectrophotometers, which was revised later (Doppler et al., 2024-Deliverable 1.2). Carvalho and Henriques (2000) retrieved AOD at 306.3, 310.0, 313.5, 316.8 and 320.0 nm using Dobson and Brewer measurements to correct for O_3 and SO_2 absorption and presented results for several days in Lisbon and Funchal, Portugal. Most AOD values at 306.3 nm were below 0.4, and Lisbon (an urban

mainland station) showed higher AOD than Funchal (an island station). They calibrated the instrument by extrapolation to zero air mass.

Gröbner et al. (2001) used an absolutely calibrated Brewer to retrieve AOD during a campaign in Huelva, Spain, in 1999 at 306, 310, 313.5, 316.75 and 320 nm by correcting for ozone absorption. Then, they transferred the calibration to six more Brewers, retrieved the AOD and compared the instruments to assess their homogeneity. Average absolute AOD differences from the first Brewer were in the range of 0.002–0.031, depending on the wavelength and the instrument.

Marenco (2002) used Langley plot calibration to retrieve AOD with a Brewer spectrophotometer in Lampedusa, Italy, by correcting for O_3 absorption through measurements made by the Brewer. The measurements were from a campaign in 2000, and AOD at 320.1 nm was mainly between 0.2 and 0.7. Comparison with retrievals from Multifilter Rotating Shadowband Radiometer (MFR-SR) AOD at 415 and 868 nm showed good correlation and mostly higher AOD at shorter wavelengths, as expected.

Kazadzis et al. (2005) retrieved AOD from a double-monochromator Brewer in Thessaloniki, Greece, using three different methods to absolutely calibrate the instrument and Langley plot calibration separately. They corrected for O_3 and SO_2 absorption through measurements made by the same instrument and compared the AOD at 355 nm with AOD from a Bentham spectroradiometer and from a multi-filter radiometer (MFR-7), showing AOD differences within 0.1 and excellent correlation (coefficient of determination $R^2 > 0.95$). Later, Fountoulakis et al. (2016) used the Brewers in Thessaloniki to study long-term trends in AOD at 320 nm, ozone and UV radiation over the period 1994–2014.

Kumharn et al. (2012) retrieved AOD from Brewers in Manchester and Reading (UK) and Selangor (Malaysia) at 320 nm and studied their climatology and variability.

More studies used Brewer measurements to retrieve AOD and validate the results with conventional instruments, which is the subject of Section 3.1.2. Below, we present in more detail the study of AOD in the UV with a Brewer spectrophotometer by Hrabčák et al. (2025). This is a newer study supported by the HARMONIA COST Action and published in the corresponding special issue.

AOD Retrieval in the UV with Brewer in Poprad-Gánovce, Slovakia

Contributor/Source: Peter Hrabčák (Hrabčák et al., 2025)

The Brewer ozone spectrophotometer at Poprad-Gánovce has provided measurements of atmospheric total ozone and ultraviolet radiation since August 1993, forming one of the longest ground-based records of its kind in Central Europe. Direct-sun observations additionally allow the retrieval of AOD in the ultraviolet spectral range. The station is located in northern Slovakia, in a predominantly rural environment influenced by the surrounding Carpathian terrain. This long-term record provides a valuable basis for assessing the seasonal variability and temporal evolution of aerosol loading under Central European conditions. AOD is retrieved using the Langley Plot Method. The resulting dataset is used to characterise the seasonal cycle and long-term changes in AOD at Poprad-Gánovce over the 1994–2025 period.

Brewer ozone spectrophotometer at the station

The Brewer ozone spectrophotometer (a single monochromator, model MKIV, No. 97) has been performing measurements at the Poprad-Gánovce station since 18 August 1993. The instrument measures direct and global UV irradiance (from 290 to 325 nm, with a step of 0.5 nm), enabling the retrieval of the total vertical columns of O_3 and SO_2, as well as a specific band in the visible suitable for NO_2 retrievals. Based on the differing absorption of radiation at these selected wavelengths, it is possible to derive the total amount of these gases in the vertical column of the atmosphere. Additionally, measurements of direct solar radiation can be used to determine AOD.

Since the beginning of its operation, daily tests have been performed on the Brewer spectrophotometer using internal lamps, and it undergoes calibration every two years. The instrument is calibrated by International Ozone Services (IOS) Inc. against the global reference group (Brewer Triad) (Fioletov et al., 2005; https://www.io3.ca/). The calibration is carried out during a calibration campaign, usually on-site or in a neighbouring country, using a travelling reference instrument, No. 17. The Brewer No. 17, used by IOS for calibrating Brewers, belongs to Environment and Climate Change Canada. When not travelling, it is stationed next to the World Brewer Reference Triad in Toronto and is frequently compared with the triad instruments. Over the years, IOS has also taken the instrument, together with

the triad instruments, to the Mauna Loa Observatory in Hawaii, USA, for independent calibrations, which have shown differences of no more than 0.5% in the total ozone column.

The measurements can be regarded as homogeneous. Occasional short interruptions occurred for technical reasons, but no extended gaps, such as entire months, are present. Regarding major technical interventions or problems, these can be summarised as follows: a secondary power supply board had to be replaced in January 2005. In February 2007, a micrometer was replaced, and during the calibration in May 2007, optical filter No. 3 was replaced, and a BM-E80 high-frequency source was also repaired.

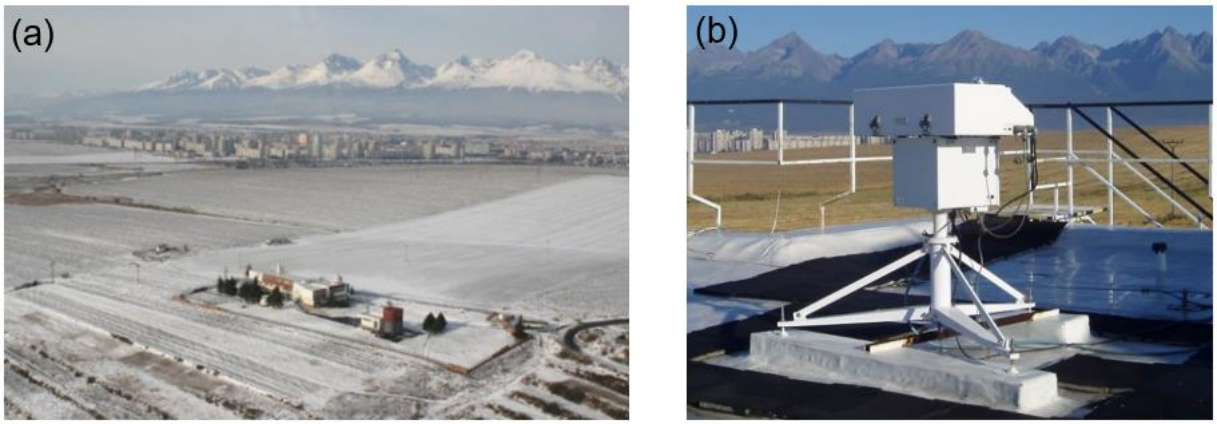


Figure 3.1: Aerial view of the Poprad-Gánovce station (a) and the Brewer ozone spectrophotometer on the station's roof (b).

Location

The Brewer spectrophotometer is located on the roof of the Aerological and Solar Radiation Center in Poprad-Gánovce, part of the Slovak Hydrometeorological Institute. Its coordinates are 49.03° N, 20.32° E (Central Europe), at an altitude of 709 m above sea level. Fig. 3.1 shows an aerial view of the Poprad-Gánovce station (a) and the Brewer ozone spectrophotometer on the station's roof (b). The view in photograph (a) is towards the northwest. The site is situated in the Podtatranská Basin, which forms part of the larger Carpathian geomorphological unit. The surrounding area includes mountain ranges of varying elevations. Gerlachovský štít

(2654 m above sea level), the highest peak in the Carpathians, is only 20 km from the station.

Local aerosol sources primarily include emissions from burning solid fuels, mainly wood, in nearby villages, as well as agricultural activities. The area experiences relatively strong winds, with prevailing wind directions from the west, north and southeast. The proximity of the city of Poprad, located approximately 1.5 km away, with a population of around 50 000 and various industrial activities, also influences the site. Despite its closeness to Poprad, the area is generally considered rural in terms of anthropogenic impact.

AOD calculation

The Brewer spectrophotometer at the Poprad-Gánovce station allows for the determination of optical depth in the UV region of the spectrum at wavelengths of 306.3, 310, 313.5, 316.8 and 320 nm. In this study, the Langley Plot Method was employed to calculate AOD. Notably, this method of AOD calculation has previously been applied to data from the Poprad-Gánovce site (Pribullová, 2002; Hrabčák, 2018). Poprad-Gánovce is neither a typical low-altitude urbanised station nor a typical high-mountain site, but rather is situated between these two cases (Hrabčák, 2018).

The contribution of sulphur dioxide (SO_2) was neglected mainly due to its low impact (Arola and Koskela, 2004) and the inaccurate determination of SO_2 at the Poprad-Gánovce station. This site is generally considered rural, with low anthropogenic influence, and SO_2 concentrations are therefore often close to the detection limit. In addition, the Brewer software settings for Poprad-Gánovce are not well optimised for the reliable retrieval of such low SO_2 values.

The air mass factor of the ozone layer was determined according to Evans and Komhyr (2008), while the air mass factor for Rayleigh scattering was determined according to Kasten and Young (1989). The air mass factor of water vapour was determined according to Kasten (1966). The air mass factor for the atmosphere as a whole was calculated as a weighted arithmetic average of the aforementioned individual components, while the optical depth of a given component was the weighting factor. Ozone absorption cross sections were taken from Gorshelev et al.

(2014) and Serdyuchenko et al. (2014) for an effective temperature of −45 °C (228.15 K) (Redondas et al., 2014). Pressure was selected through interpolation based on three daily measurements in local climatic terms. The optical depth of Rayleigh scattering was calculated according to Bodhaine et al. (1999). The Langley calibration methodology was a modified version of Hrabčák (2018). The AOD threshold at 320 nm was reduced from 0.5 to 0.4, the standard deviation of the daily ozone column was relaxed from < 2.5 DU to < 3 DU, the standard deviation of the daily AOD was tightened from < 0.07 to < 0.04, and the required coefficient of determination (R^2) of the linear interpolation was increased from > 0.98 to > 0.99.

Raw data post-processing

The raw signals were corrected for the instrument dead time and temperature dependence, including a spectral transmittance correction for the neutral density filter according to SCI-TEC Instruments Inc. (1999) and a correction for the stray-light effect according to Garane et al. (2006). The methodology of the given correction in the case of the Brewer at the Poprad-Gánovce station is described in more detail in Hrabčák (2018). The impact of polarisation was compensated for according to Hrabčák (2018). The correction for the impact of diffuse radiation follows the recommendations of Arola and Koskela (2004). The instrument takes five consecutive measurements, each lasting approximately half a minute, resulting in five AOD values in less than 2 minutes. The final AOD for each measurement is the arithmetic mean of the five values. All final AOD values underwent a quality control procedure, including cloud screening, according to Hrabčák (2018).

Brief overview of measurement results

The long-term monthly characteristics of AOD at 320 nm, slightly extended compared to the published study (Hrabčák et al., 2025), are presented in Fig. 3.2. The analysis covers the 32-year period (1994–2025). We can observe a bimodal annual cycle, with the first peak occurring in April and the second, more pronounced peak in August. The lowest values in the long-term average are observed in December.

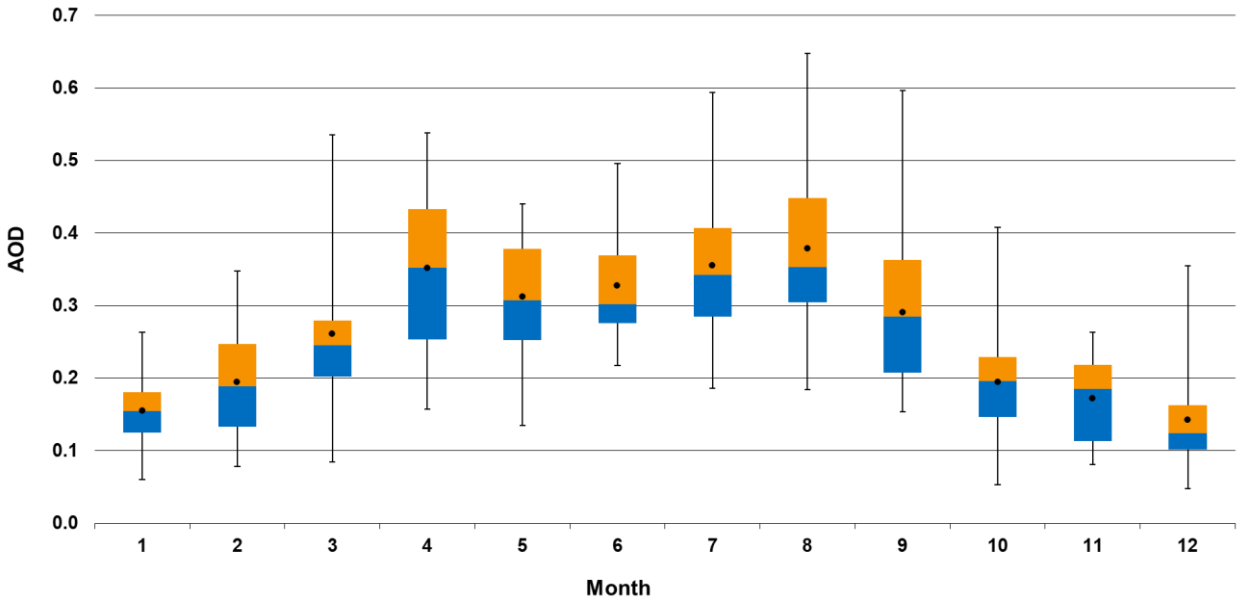


Figure 3.2: The long-term monthly characteristics of AOD at 320 nm for Poprad-Gánovce obtained over the 32-year period (1994–2025). Solid points indicate mean values, the line inside the boxes represents the median, the box limits correspond to the first (25%) and third (75%) quartiles, and the whiskers indicate the minimum and maximum values.

The long-term trend can be clearly seen in Fig. 3.3, which compares the annual mean AOD at the two Brewer wavelengths and their linear trends over the 32-year period. A statistically significant gradual decrease in AOD is evident at both wavelengths. The overall change over 32 years, according to the linear fit, is −0.18 at 320 nm and −0.17 at 316.8 nm. The results fit well into the overall picture of recent AOD trends across the wider Central European region. Until recently, the lowest annual mean values were observed in 2020, during the first year of the COVID-19 pandemic. However, 2025 recorded even lower AOD values at both wavelengths.

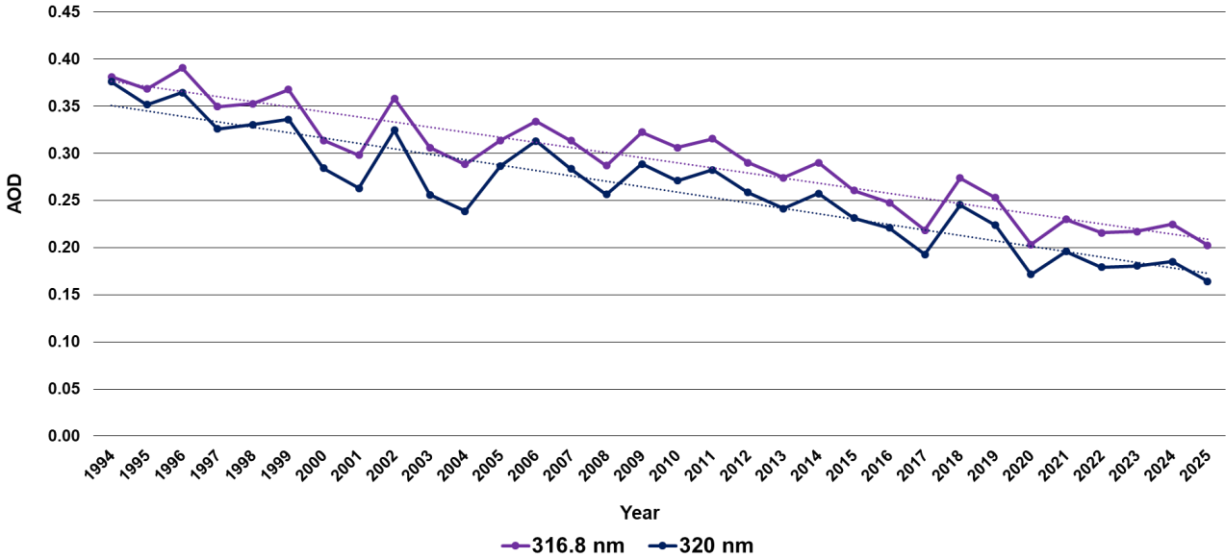


Figure 3.3: Comparison of annual mean AOD at the two longest Brewer wavelengths and their linear trends in Poprad-Gánovce over the 32-year period (1994–2025).

3.1.2 Validation of AOD from UV spectroradiometers

As we showed earlier, Gröbner et al. (2023) performed a comparison of AOD from spectroradiometers covering the range from the near-UV to the near-IR with reference filter radiometers. Several previous studies have examined the accuracy of AOD in the UV using such comparisons, and we provide an overview below.

Gröbner and Meleti (2004) retrieved AOD in the 306–320 nm range using a Brewer in Ispra, Italy, during 1991–2002 and studied its climatology and drivers. They used absolute calibration and a satellite extraterrestrial solar spectrum. They corrected the AOD for O_3 and NO_2 absorption measured by the Brewer and showed excellent correlation between Brewer AOD at 320 nm and CIMEL at 340 nm. Brewer AOD was systematically higher, as expected due to the shorter wavelength.

Kazadzis et al. (2007) studied the climatologies and compared AOD from Brewers in Thessaloniki, Greece, at 320 and 340 nm with AERONET, showing good correlation. A newer study, Fountoulakis et al. (2019), retrieved AOD, absorption AOD and single scattering albedo (SSA) at 320, 340 and 360 nm from the Brewers in the same location and studied the climatologies during the period 2005–2017. The comparison of AOD with AERONET at 340 nm showed average differences mostly within 0.01.

De Bock et al. (2010) retrieved AOD with a Brewer at Uccle, Belgium, at 340 nm and compared it with AERONET AOD at the same wavelength, showing excellent correlation.

Kumharn et al. (2015) studied the variability of AOD at 320 nm in Bangkok and Songkhla and compared the results with AERONET AOD scaled to the same wavelength, showing good correlation (R^2 = 0.89).

López-Solano et al. (2018) retrieved AOD from various Brewers within the European Brewer Network (EUBREWNET) with an algorithm intended to be applied throughout the network and therefore to provide better homogeneity. They used AERONET and UVPFR as references to validate the AOD at 306.3, 310.1, 313.5, 316.8 and 320.1 nm. Median differences were mostly below 0.01, standard deviations were below 0.03, and correlation factors were above 0.95, showing good consistency in comparisons with both UVPFR and AERONET AOD extrapolated to 320 nm.

Overall, despite the challenges, several studies show encouraging results for AOD observations in the UV, as long as ozone absorption is not too strong and all necessary gases are considered according to the conditions at the location. The methodology is currently operational in EUBREWNET (Doppler et al., 2024-Deliverable 1.2).

3.2 Spectral AOD retrievals in VIS and IR

Visible

The visible is a narrow spectral region where gas absorptions are limited and the conventional filter radiometers measure at different wavelengths (500 nm — all 3 networks, 400 nm — SKYNET, 412 nm — GAW-PFR, 440 and 675 nm — AERONET). Certain spectroradiometers can also provide AOD in the region, and below we show some examples of related studies.

Diémoz et al. (2016) used a modified Brewer version in Athens, Greece, that includes measurements in the visible, one of its channels being 437 nm, and is therefore suitable for validation of AOD in Athens against CIMEL at 440 nm during the period 2008–2014. The results showed good correlation and no obvious strong bias, but the standard deviation was large (0.05), with only 37% of the coincident data within the

WMO limits (95% is required for the WMO traceability criterion). Moreover, the differences showed a statistically significant trend of 0.003 per year, attributed to Brewer instability.

A recent work related to a HARMONIA virtual mobility (Anyfanti, 2026) included AOD retrieval at 320 and 442.9 nm from the same spectrophotometer (Brewer in Athens). It also included a comparison with AERONET AOD at 320 and 440 nm and AE for the 340–440 nm pair during a campaign in Thessaloniki in September 2026. The comparison at 440 nm showed a significant bias towards higher Brewer AOD (mean AOD difference 0.028), while the standard deviation around it was below 0.01 and would allow 82% of differences to be within the WMO limits if the bias was 0. At 320 nm, the mean difference was 0.033 towards higher Brewer AOD, the standard deviation was 0.016, and 60% of the data points would be within the WMO limits under a bias of 0. Calibration bias is suspected as the cause of these biases. The AE differences were within 0.4.

Infrared

AOD in the IR is typically provided at 862/870 and 1020 nm by the sun photometric networks. The wavelengths 862 and 870 nm are two particularly suitable wavelengths, to the extent that AERONET corrects 870 nm only for Rayleigh scattering (Giles et al., 2019). The 1020 nm channel includes very weak absorption, mostly from water vapour. AERONET provides measurements at 1640 nm, which is not as widely available or studied as the aforementioned wavelengths, and the rest of the IR is not so well studied, while studies of such AOD retrievals from spectroradiometers are limited.

Kudo et al. (2021) used sky radiance measurements from Tsukuba, Japan, to retrieve AOD at all wavelengths of the SKYNET POM-02 instruments, which include 1627 and 2200 nm channels.

Gröbner et al. (2024) compared retrievals at 1020 and 1640 nm between AERONET, BTS observations and extrapolated AOD from BTS and PFR. The differences were mostly below 0.01 or 0.02, but in certain cases showed systematic bias, pointing to the possibility of features of AOD in that region that deviate from the law, errors in gas correction or calibration discrepancies.

Other studies have focused on AOD retrievals from different instrument types, which rely on interferometry, mostly Fourier-transform infrared spectrometers (FTIRs).

Ritter et al. (2005) used FTIR measurements from Koldewey station in Ny-Ålesund/Spitsbergen, Norway, during polar nights (terrestrial radiation measurements) in 1995 and 1997. They retrieved AOD in the thermal infrared (approximately 8 to 14.3 μm), which was 0.04 on average.

Thomas et al. (2009) used FTIR measurements of solar radiation from Puerto Rico and Senegal during desert dust episodes in 2006. The AOD measurements covered the spectral region between 8 and 13 μm. In certain cases, AOD exceeded 0.5, while a co-located CIMEL showed AOD > 1 at 670 nm. Comparison with modelled AOD from Mie calculations showed a similar peak of AOD above 8 μm at 9.5 μm and differences that depended on the size distribution provided as input to the model.

Barreto et al. (2020) used an FTIR at Izaña Observatory, Tenerife, Spain, from May 2019 to May 2020. They selected seven narrow spectral bands centred at 1020.9, 1238.25, 1558.25, 1636, 2133.4, 2192 and 2314.2 nm with minimal gas absorption, averaged the measured radiation within each band and retrieved AOD. They also used the filter response function of AERONET to convolve the FTIR spectrum (which has a higher resolution and narrower bandwidth than CIMEL's) at the directly comparable channels (1020 and 1640 nm). The FTIR was calibrated with the Langley plot method. To calculate AOD, they corrected for the gas absorptions of H_2O, CO_2 and CH_4 (FTIRs primarily measure greenhouse gases). Mean AOD differences between CIMEL and FTIR in the common channels were below 0.004, and root mean squared errors were below 0.006. However, the 1640 nm channel showed a systematic bias towards higher AOD than CIMEL. AE in this region was typically below 0.6, often close to 0 during dust episodes. For very low AOD (background conditions), it showed larger variability, which was a result of the high sensitivity of AE at low aerosol loads and the power-law fitting to the Ångström law under conditions in which spectral AOD in this region was very low and flat.

Alvárez et al. (2023) also used a portable low-resolution FTIR in Izaña during 2019–2022 to retrieve AOD in the 873–2314 nm range and compare it with AERONET AOD,

showing good agreement (mean AOD differences up to 0.005, standard deviations up to 0.021 and correlation coefficients up to 0.97).

Frausto-Vicencio et al. (2023) used the methodology of Barreto et al. (2020) to measure AOD at narrow bands centred at 1020.9, 1238.25, 1558.25 and 1636 nm with an FTIR in the San Joaquin Valley during the 2020 wildfire season, with measurements of smoke plumes from the Sierra Nevada of California. They showed a slight correlation between AOD and carbon monoxide (CO) concentration.

Ji et al. (2026) used CIMEL and FTIR measurements in Ny-Ålesund, assimilated AOD for different aerosol types, forward modelling and machine learning to study aerosol composition. The FTIR provided ground-based AOD observations at 1020.9, 1238.25, 1558.25, 2133.40, 2192 and 2314.2 nm.

Seo et al. (2022) used the Atmospheric Emitted Radiance Interferometer (AERI) in Anmyeon, South Korea, which is a Fourier-transform spectrometer that measures downwelling radiance at 3.3–18.2 μm. They retrieved AOD at 500 nm through the use of the vertical structure of temperature and water-vapour mixing ratio (also retrieved from the instrument), radiative transfer modelling and an inversion technique. They compared the results with a co-located PFR and showed a similar variation, but systematically lower AOD.

Wider range

Gröbner and Kouremeti (2019) used a PSR to retrieve AOD from the UV to the near-IR in Davos, Switzerland, and showed good agreement at the common wavelengths with AOD from the PFR triad, which is the WMO reference for AOD, as did Gröbner et al. (2023). The PSRs also participate in the Filter Radiometer Comparison (FRC) campaign, which includes such comparisons (Kazadzis et al., 2023).

In a more recent study, published in the HARMONIA COST Action special issue, Karanikolas et al. (2025) used AOD (UV to near-IR) from a PFR and a double BTS spectroradiometer calibrated in SI units to retrieve the aerosol size distribution through inverse modelling. The study investigated the effect of spectral range, using 5 BTS wavelengths in the 1022–2130 nm range after applying a correction for greenhouse gases, and showed reasonable size distribution retrievals that would be expected under reliable and not heavily biased AOD. More details about this work

and the AOD correction method are in Karanikolas (2026). Section 4 focuses on those AOD retrievals from BTS; therefore, the discussion will be more detailed there.

3.3 AOD retrieval from MAX-DOAS instruments

Certain spectroradiometers, such as Pandora (Liu et al., 2024), are used to retrieve trace gases with the MAX-DOAS method. They mostly measure sky radiance and are not calibrated in SI units, nor are they usually calibrated with the Langley method. Yet, AOD and aerosol properties can be retrieved with alternative methodology. Those instruments usually cover parts of the UV and visible spectral regions. Pandora, for example, measures in the 280–525 nm range.

Wagner et al. (2004) and Friess et al. (2006) presented a methodology that uses the differential absorption of the oxygen dimer O_4 to retrieve aerosol properties, including AOD and the vertical profile of aerosols. This methodology uses the spectra measured by MAX-DOAS instruments at different angles and does not require radiometric calibration.

Clémer et al. (2010) applied the method to a MAX-DOAS instrument in Beijing, China, during 2008–2009 at four wavelengths—360, 477, 577 and 630 nm—to retrieve AOD and the aerosol vertical profile. They also compared the AOD with AERONET AOD scaled to the wavelengths of the MAX-DOAS instrument. The results showed very good correlation for the two shortest wavelengths, while for the other two, the correlation factor dropped below 0.7. There was also an increasing tendency for MAX-DOAS AOD to be lower than AERONET AOD at higher AOD values.

Karagkiozidis et al. (2022) used the technique with MAX-DOAS instruments in Thessaloniki, using two different algorithms at 360 and 477 nm. They compared the results with each other and with AOD from Brewer and CIMEL and tested different schemes for cloud screening and quality control. The results showed variable performance based on the algorithm and data selection. The correlation factors with CIMEL or Brewer were up to 0.8.

4. Spectral AOD with high spectral range and resolution

In this section we provide a few examples and some discussion on AOD retrievals from high spectral range and resolution using a double BTS spectroradiometer used by PMOD/WRC in Davos, Switzerland (Fig. 4.1). The 2 instruments measure in parallel, with the first BTS measuring in the 300-1050 nm range and the second in the 950-2150 nm range (Karanikolas et al., 2025). We use the second spectroradiometer for all wavelengths above 1000 nm creating a merged dataset between them with no spectral overlap. The location is at nearly 1600 m in the Eastern Swiss Alps. The conditions are typically pristine with occasional Saharan dust episodes or intrusions of anthropogenic pollution and wildfire smoke. More details for the location and instrumentation are available in Karanikolas et al. (2025).

4.1 Methodology

The instruments are calibrated in SI units at Physikalisch-Technische Bundesanstalt (PTB), Germany. The extraterrestrial spectrum was TSIS-1 Hybrid Solar Reference Spectrum (HSRS) (Richard et al., 2020) convoluted for the slit function of the BTS. This allows the calculation of the total optical depth. Rayleigh scattering is corrected with the method of Bodhaine et al. (1999) and ozone absorption with the cross sections of Serdychenko et al. (2014). The total column of ozone is available from a co-located Brewer spectrophotometer. To remove residual absorptions from the BTS optical depth datasets we used the model uvspec from the libradtran package (Emde et al., 2016) according to Karanikolas (2026) (variable H_2O, any other gas fixed). For most of the wavelengths presented below such correction is negligible (<0.001). For wavelengths in the 1022–1551 nm range the corrections were above 0.001, but below 0.01 for typical conditions in Davos, while the two channels above 2100 nm may require correction exceeding 0.01 or even 0.02 (Karanikolas, 2026). The total column of H_2O in this deliverable was available through BTS retrievals and therefore simultaneous to the optical depths, so we did not use the AERONET one in this case. For CO_2, CH_4 and N_2O we used the global average of NOAA according to Karanikolas (2026).

We selected the presented wavelengths manually by avoiding strong gas absorptions and channels showing significantly higher discrepancy from the Ångström law compared to their nearby wavelengths. The examples and statistics show 2 wavelength selections:

1. Long spectral range: 16 wavelengths in the 340–2130 nm range (Karanikolas et al., 2025).
2. High spectral resolution: 496 wavelengths in the 334.6–872.5 nm range.

To compare the observed AOD with that predicted by the Ångström law we used a linear fit on the logarithms of all common wavelengths of BTS with CIMEL and PFR (Karanikolas et al., 2025).

As the instrument currently includes no operational procedures for cloud screening and quality assurance, we used the comparison with a co-located PFR (Karanikolas et al., 2025). The dataset used here includes 17637 observations in the 2023–2025 period.



Figure 4.1: BTS spectroradiometers in PMOD/WRC, Davos.

4.2 Results and discussion

The statistics of the differences between observed and predicted AOD (Fig. 4.2) show very similar results to those in Karanikolas et al. (2025), although the dataset is a subset and H_2O correction is through BTS measurements instead of CIMEL, showing that there are quite systematic features. In the high spectral range selection (panel a), the spectral region between 675–870 nm shows very smooth behaviour and is very close to the Ångström law. The same is true for the region 600–870 nm in the case of high spectral resolution (panel b). Above 1000 nm the deviations gradually increase towards the longer wavelengths (although 1238 nm shows a larger deviation than 1551 nm). In the case of high spectral resolution, the statistics are more 'noisy' below 550 nm and even more below 490 nm.

There are different explanations for discrepancies from the Ångström law:

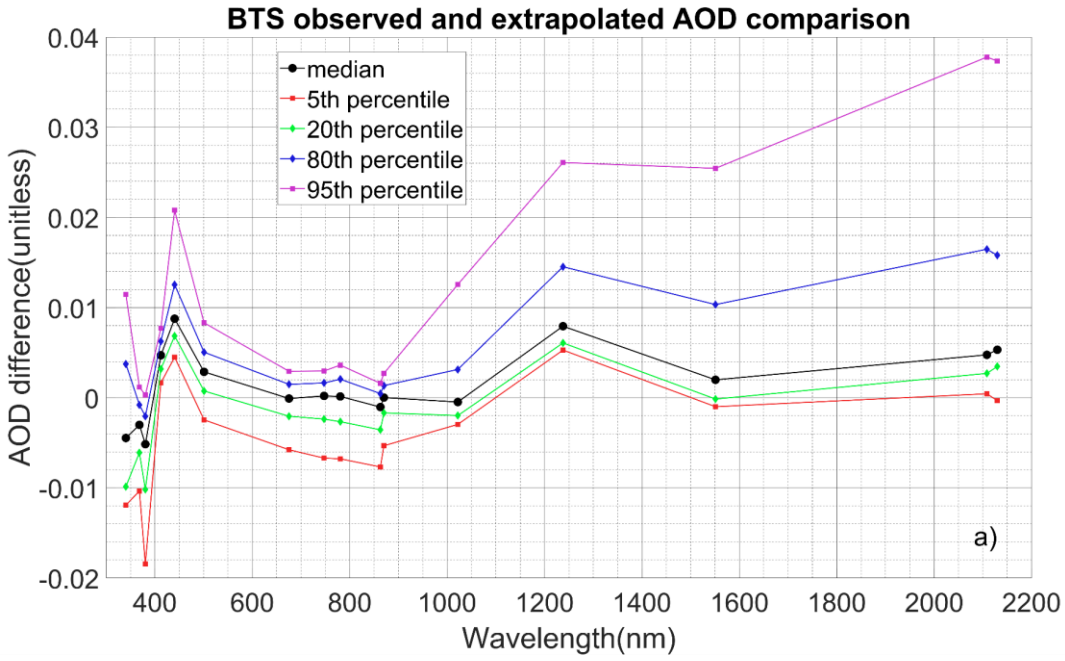
1. Spectral AOD features that the Ångström law does not predict.
2. Errors in the correction of gas absorption.
3. The effect of slit function: errors in convolution of the extraterrestrial spectrum, incompatibilities with the ground-based spectrum, and strong lines of the solar spectrum.
4. AOD uncertainties due to other factors such as the raw signal noise or calibration.

Explanation 2 should concern the 2 longest wavelengths where the absorption of H_2O is stronger. Beyond that, certain wavelengths may include narrow absorption lines where the parametrisation of uvspec and the convolution may have failed to account for them properly. Explanation 4 describes random uncertainties plus the calibration, which can be randomly higher or lower than the 'true' value for each wavelength, but may remain the same or similar for a large period of time creating systematic offsets. The spectral region between 335–550 nm is one of the least affected by gas absorption and the most typical in the application of the Ångström law in the general case (a special episode is included below). Yet, it is affected by stronger consistent discrepancies among all percentiles between wavelengths differing even by less than 1–2 nm, without smooth features. Therefore, we expect that the effect of the slit function is stronger in that case and explains most of this behaviour.

The 4 wavelengths above 1022 nm are systematically above the Ångström law (although not always) with the 80th percentile exceeding 0.01. This could be a result of systematic error in gas absorption corrections or a result of the Ångström law being unsuitable to describe AOD in the region. In Karanikolas et al. (2025) this increased AOD did not result in systematically higher coarse mode volume concentration compared to AERONET. This parameter is particularly sensitive in the longest wavelengths and the use of AOD without the correction for greenhouse gases strongly affects the coarse mode concentration retrieved by GRASP. Using the corrected AOD removed this bias, providing some evidence that the systematic bias is not significant. However, this is dependent on the way GRASP models aerosols

and the AERONET observations for validation were limited, so our results are not conclusive.

The median differences between BTS and PFR at common wavelengths for the dataset used here were below 0.006 (below 0.004 for the 3 longest ones) and the absolute values of the 5th and 95th percentiles were below 0.02 (up to 0.01 for the 3 longest ones).



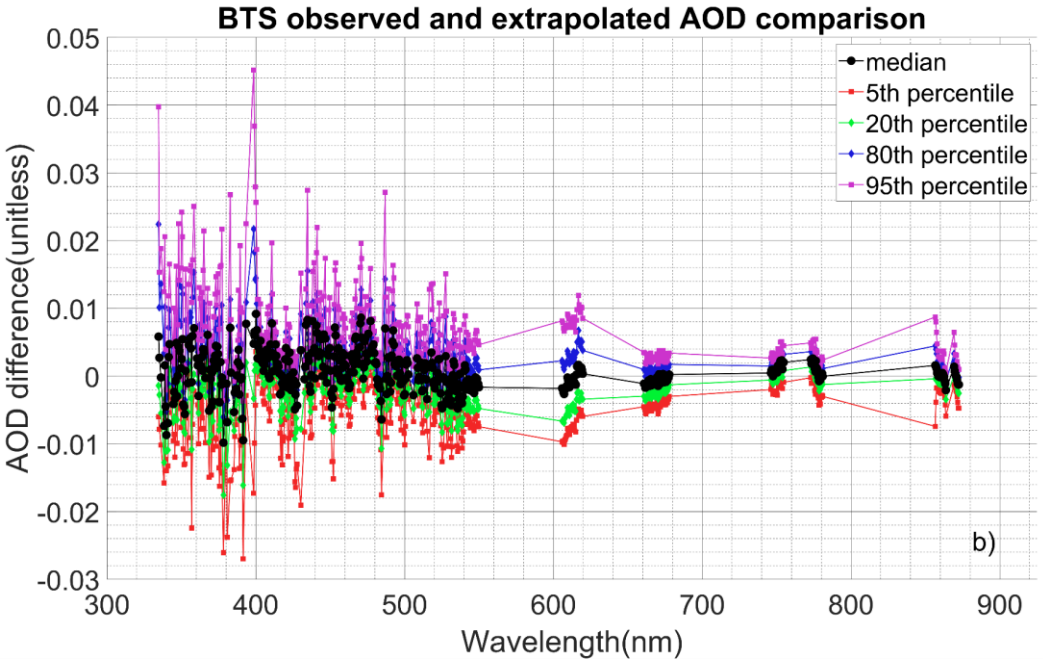


Figure 4.2: Statistics of AOD differences between observed and predicted AOD from 17637 BTS observations in the 2023–2025 period. Panel a shows 16 selected wavelengths in the full range of the instrument and panel b 496 selected wavelengths below 875 nm.

Aside from the statistics, we provide a few examples of single measurements showing the behaviour of AOD in each of the 2 wavelength selections. The first example is from 28th October 2024 where the conditions are quite typical for the location. AOD is below 0.07 even at 340 nm (Fig. 4.3). The comparison with the Ångström law shows some of the 'features' present in Fig. 4.1, although the calculation of the Ångström exponent (only common wavelengths with CIMEL and PFR) shows high goodness of fit (R^2=0.94). Generally, the wavelengths do not follow any smooth function well. Repeating the analysis after Langley plot calibration and re-calculation of AOD (so the slit function of both extraterrestrial and measured at the surface irradiances) would provide useful insights on how much smoother the spectral AOD can get both statistically and spectrum by spectrum. However, wavelengths being too close to each other results in AOD uncertainty being higher than AOD spectral change and therefore if spectral resolution is too high, such phenomena will be at least partially retained.

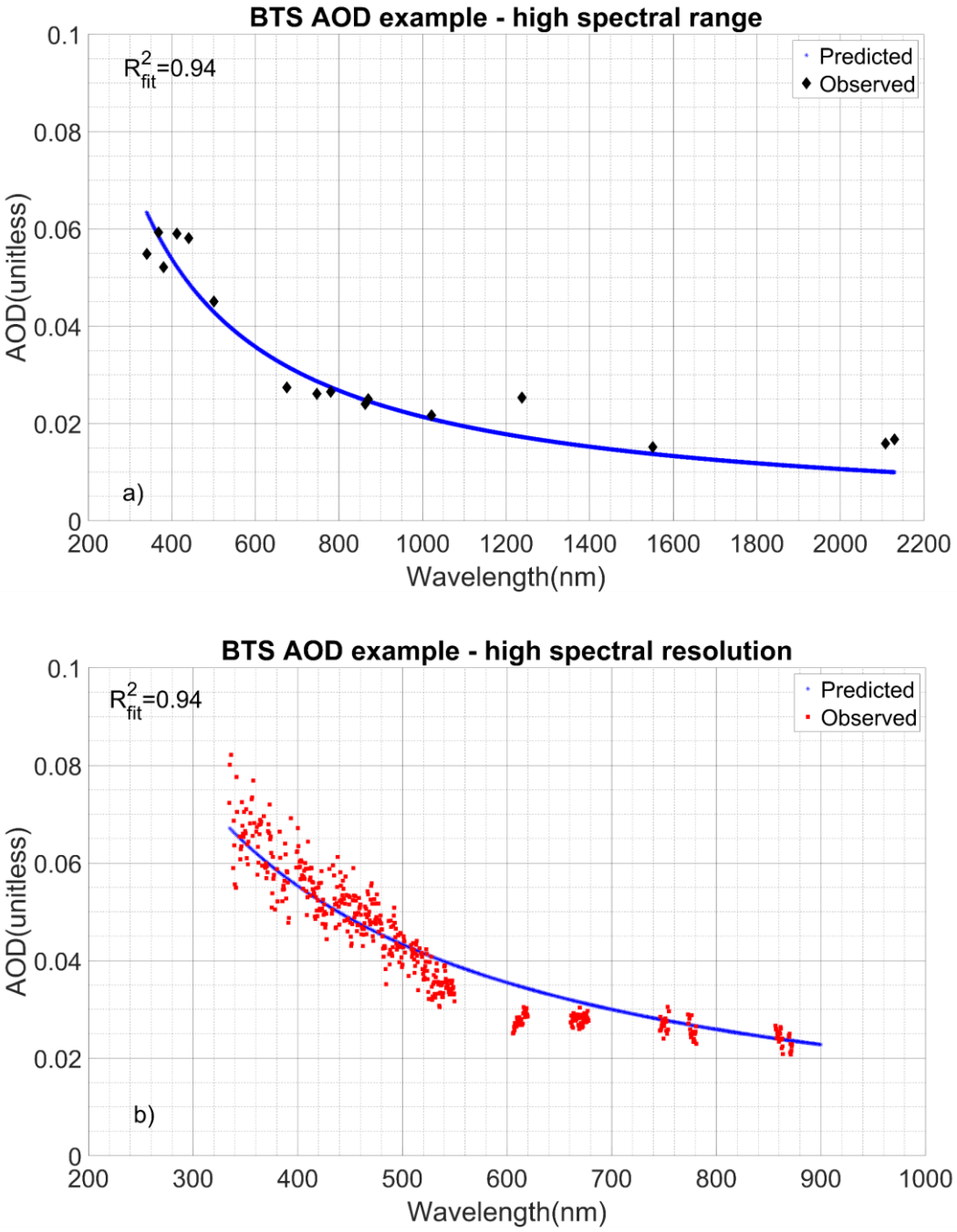


Figure 4.3: Example of AOD retrievals from BTS in Davos on 28/10/2024 at 12.85 UTC. Panel a shows the 16 selected wavelengths over the entire range and panel b the high-resolution retrievals below 900 nm.

The second example concerns a dust episode (although not a very strong one that would correspond to a very small Ångström exponent). Dust episodes in Davos are

limited, often accompanied by clouds, and it was challenging to find episodes under clear sky within the dataset, which covers part of 3 years. This analysis would be interesting in a more suitable location such as Izaña, Tenerife. Fig. 4.4 shows similar features to Fig. 4.3 although not identical. The goodness of fit is lower in this case.

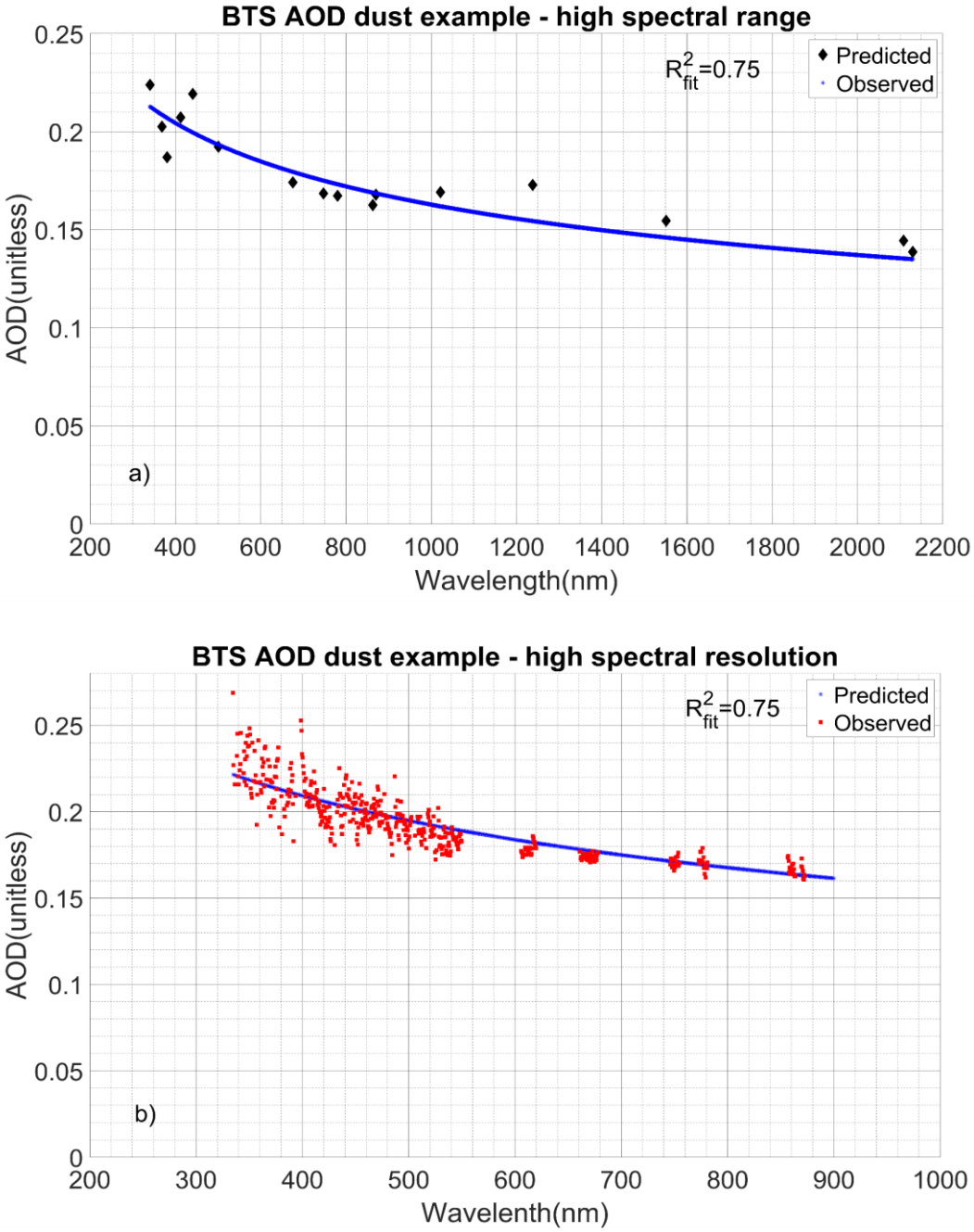


Figure 4.4: Example of AOD retrievals from BTS in Davos on 19/6/2024 at 9:10 UTC, during transport of Saharan dust to the Alps. Panel a shows the 16 selected

wavelengths over the entire range and panel b the high-resolution retrievals below 900 nm.

The final example concerns an unusually long-range transport of smoke from Canadian wildfires to Europe during autumn 2023. The measurement is from 1st October 2023 and shows a quite consistent tendency for a negative Ångström exponent up to 500 nm. This was visible in PFR and CIMEL AOD at the same time in the same location, but also at different AERONET stations before or after that day (Masoom et al., 2026; Karanikolas et al., 2025). The analysis of those studies showed an unusual size distribution both in retrievals from sky radiance inversions or AOD only, which showed a dominant fine mode of unusually large particles for fine mode and coarse mode concentration close to 0. Fig. 4.5 shows that the spectral behaviour is visible even in the case of high spectral resolution since most wavelengths below 450 nm show lower AOD than most of those in the 450–550 range. Although the AOD peaks above 0.5, the AOD in the IR drops below 0.15 or even below 0.1. Therefore, the Ångström exponent between very short and very long wavelengths is large as typically happens during fine mode dominated conditions.

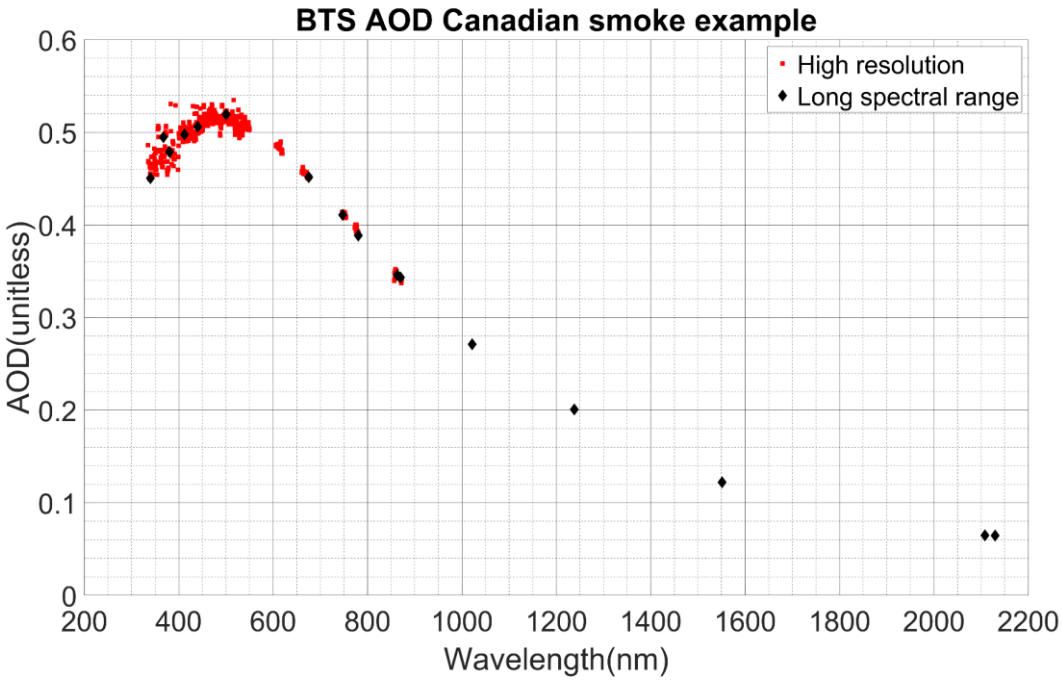


Figure 4.5: Example of AOD retrievals from BTS in Davos on 1/10/2023 at 10:00 UTC, during transport of smoke from Canadian wildfires to Europe. The black diamonds show the 16 selected wavelengths over the entire range and the red squares the high-resolution retrievals below 900 nm.

5. Summary

There are various studies showing that AOD is retrievable from different spectroradiometers even beyond the conventionally used wavelengths by filter radiometers. Comparisons between them at the common wavelengths showed generally good agreement. Certain cases of larger differences could be explained by calibration errors or technical issues or imperfect cloud screening. Yet there are remaining challenges, particularly for absolutely calibrated instruments, and even more so, in wavelengths beyond the common ones between spectroradiometers and filter radiometers. More research is required to optimise the wavelength selections and retrievals per instrument, including corrections for gas absorptions and instrument slit functions.

The high resolution of spectroradiometers provides flexibility to improve wavelength selection. However, attempting to take full advantage of the spectral resolution results in wavelength-to-wavelength differences that can be driven more by uncertainty or biases than by real AOD changes if the channels are too close to each other. An optimal selection of a limited number of wavelengths over the entire range can show more accurately the spectral dependence of AOD. Particularly, instruments such as the combination of two co-located BTS spectroradiometers with different spectral ranges measuring synchronised and treated as one instrument, with common procedures, can result in a homogenised AOD dataset that shows the AOD spectral dependence from the UV to the IR beyond 2100 nm.

HARMONIA enabled comparative studies in two ways. First, it strengthened collaboration among the spectroradiometer and photometer (filter radiometer) communities. Second, a range of grants provided financial support for research publications, virtual mobility for comparison studies, short-term scientific missions (STSMs) to participate in campaigns and training, and experimental exchanges. This support helped overcome boundaries between networks and manufacturers, encouraging researchers to share data, methods, and measurements. The resulting cross-comparisons made it possible to assess the quality of different systems and methods objectively and scientifically—and, ultimately, to improve them.

References

Alvárez, Ó., Barreto, Á., García, O. E., Hase, F., García, R. D., Gröbner, J., León-Luis, S. F., Sepúlveda, E., Carreño, V., Alcántara, A., Ramos, R., Almansa, A. F., Kazadzis, S., Taquet, N., Toledano, C., and Cuevas, E.: Aerosol properties derived from ground-based Fourier transform spectra within the COllaborative Carbon Column Observing Network, Atmos. Meas. Tech., 16, 4861–4884, https://doi.org/10.5194/amt-16-4861-2023, 2023.

Andrews, A. E., Kofler, J. D., Trudeau, M. E., Williams, J. C., Neff, D. H., Masarie, K. A., Chao, D. Y., Kitzis, D. R., Novelli, P. C., Zhao, C. L., Dlugokencky, E. J., Lang, P. M., Crotwell, M. J., Fischer, M. L., Parker, M. J., Lee, J. T., Baumann, D. D., Desai, A. R., Stanier, C. O., De Wekker, S. F. J., Wolfe, D. E., Munger, J. W., and Tans, P. P.: CO2, CO, and CH4 measurements from tall towers in the NOAA Earth System Research Laboratory's Global Greenhouse Gas Reference Network: instrumentation, uncertainty analysis, and recommendations for future high-accuracy greenhouse gas monitoring efforts, Atmos. Meas. Tech., 7, 647–687, https://doi.org/10.5194/amt-7-647-2014, 2014.

Anyfanti, K.: Evaluation the spectral AOD from the MKIV Brewer#001 spectrophotometer through intercomparison with multiple sensors in Thessaloniki, Greece, Virtual mobility report, HARMONIA COST action, CA21119, 2026.

Arola, A. and Koskela, T.: On the sources of bias in aerosol optical depth retrieval in the UV range, J. Geophys. Res., 109, D08209, https://doi.org/10.1029/2003JD004375, 2004.

Barreto, Á., García, O. E., Schneider, M., García, R. D., Hase, F., Sepúlveda, E., Almansa, A. F., Cuevas, E., and Blumenstock, T.: Spectral Aerosol Optical Depth Retrievals by Ground-Based Fourier Transform Infrared Spectrometry, Remote Sens., 12, https://doi.org/10.3390/rs12193148, 2020.

Bodhaine, B. A., Wood, N. B., Dutton, E. G., and Slusser, J. R.: On Rayleigh Optical Depth Calculations, J. Atmos. Ocean. Tech., 16, 1854–1861, https://doi.org/10.1175/1520-0426(1999)016<1854:ORODC>2.0.CO;2, 1999.

Carlund, T., Kouremeti, N., Kazadzis, S., and Gröbner, J.: Aerosol optical depth determination in the UV using a four-channel precision filter radiometer, Atmos. Meas. Tech., 10, 905–923, https://doi.org/10.5194/amt-10-905-2017, 2017.

Carvalho, F. and Henriques, D.: Use of Brewer ozone spectrophotometer for aerosol optical depth measurements on ultraviolet region, Adv. Space Res., 25, 997–1006, 10.1016/S0273-1177(99)00463-9, 2000.

Clémer, K., Van Roozendael, M., Fayt, C., Hendrick, F., Hermans, C., Pinardi, G., Spurr, R., Wang, P., and De Mazière, M.: Multiple wavelength retrieval of tropospheric aerosol optical properties from MAXDOAS measurements in Beijing, Atmos. Meas. Tech., 3, 863–878, https://doi.org/10.5194/amt-3-863-2010, 2010.

Cuevas, E., Romero-Campos, P. M., Kouremeti, N., Kazadzis, S., Räisänen, P., García, R. D., Barreto, A., Guirado-Fuentes, C., Ramos, R., Toledano, C., Almansa, F., and Gröbner, J.: Aerosol optical depth comparison between GAW-PFR and AERONET-Cimel radiometers from long-term (2005–2015) 1 min synchronous measurements, Atmos. Meas. Tech., 12, 4309–4337, https://doi.org/10.5194/amt-12-4309-2019, 2019.

De Bock, V., De Backer, H., Mangold, A., and Delcloo, A.: Aerosol Optical Depth measurements at 340 nm with a Brewer spectrophotometer and comparison with Cimel sunphotometer observations at Uccle, Belgium, Atmos. Meas. Tech., 3, 1577–1588, https://doi.org/10.5194/amt-3-1577-2010, 2010.

Diémoz, H., Eleftheratos, K., Kazadzis, S., Amiridis, V., and Zerefos, C. S.: Retrieval of aerosol optical depth in the visible range with a Brewer spectrophotometer in Athens, Atmos. Meas. Tech., 9, 1871–1888, https://doi.org/10.5194/amt-9-1871-2016, 2016.

Doppler, L., Karanikolas, A., Garcia Suñer, M., Kumar, G., Kazadzis, S., and Kouremeti, N.: Differences and harmonization possibilities in AOD retrieval methods, COST ACTION, COST-EUROPEAN COOPERATION IN SCIENCE AND TECHNOLOGY, Brussels, Belgium, COST CA21119 HARMONIA-WG1 Deliverable-D1.3, submitted in October 2026.

Doppler, L., Akriti M., Barreto Velasco, A., Estellés, V., Fountoulakis, I., Frangipani, C., Gonzalez Sicilia, P., Graßl, S., Hrabčák, P., Ivanescu, L., Karanikolas, A., Kazadzis, S.,

Kouklaki, D., Kouremeti, N., Kumar, G., Laguarda Cirigliano, A., Mangold, A., Román Diez, R., Russo Ganón, P., Savastiouk, V. and Zuber, R.: Differences and harmonization possibilities in AOD retrieval methods, COST ACTION, COST-EUROPEAN COOPERATION IN SCIENCE AND TECHNOLOGY, Brussels, Belgium, https://harmonia-cost.eu/wp-content/uploads/2024/12/Harmonia_D1.2_ver2.pdf (last access: 20 September 2026), 2024.

Doppler, L., Akriti Masoom, A., and Karanikolas, A.: Create a list of existing and foreseen campaigns or experiments needed for night and day aerosol measurements and report on the data collection and analysis of the data/measurements, COST ACTION, COST-EUROPEAN COOPERATION IN SCIENCE AND TECHNOLOGY, Brussels, Belgium, https://harmonia-cost.eu/wp-content/uploads/2023/10/COST_CA21119_HARMONIA-WG1_Deliverable-D11.pdf (last access: 20 September 2026), 2023.

Drosoglou, T., Raptis, I.-P., Valeri, M., Casadio, S., Barnaba, F., Herreras-Giralda, M., Lopatin, A., Dubovik, O., Brizzi, G., Niro, F., Campanelli, M., and Kazadzis, S.: Evaluating the effects of columnar NO2 on the accuracy of aerosol optical properties retrievals, Atmos. Meas. Tech., 16, 2989–3014, https://doi.org/10.5194/amt-16-2989-2023, 2023.

Fioletov, V. E., Kerr, J. B., McElroy, C. T., Wardle, D. I., Savastiouk, V., and Barton, D. N.: The Brewer reference triad, Geophys. Res. Lett., 32, L20805, 10.1029/2005GL024244, 2005.

Fountoulakis, I., Bais, A. F., Fragkos, K., Meleti, C., Tourpali, K., and Zempila, M. M.: Short- and long-term variability of spectral solar UV irradiance at Thessaloniki, Greece: effects of changes in aerosols, total ozone and clouds, Atmos. Chem. Phys., 16, 2493–2505, https://doi.org/10.5194/acp-16-2493-2016, 2016.

Fountoulakis, I., Natsis, A., Siomos, N., and Bais, A.: Deriving Aerosol Absorption Properties from Solar Ultraviolet Radiation Spectral Measurements at Thessaloniki, Greece, Remote Sens., 11, 2179, https://doi.org/10.3390/rs11182179, 2019.

Frausto-Vicencio, I., Heerah, S., Meyer, A. G., Parker, H. A., Dubey, M., and Hopkins, F. M.: Ground solar absorption observations of total column CO, CO2, CH4, and aerosol optical depth from California's Sequoia Lightning Complex Fire: emission

factors and modified combustion efficiency at regional scales, Atmos. Chem. Phys., 23, 4521–4543, https://doi.org/10.5194/acp-23-4521-2023, 2023.

Friess, U., Monks, P. S., Remedios, J. J., Rozanov, A., Sinreich, R., Wagner, T., and Platt, U.: MAX-DOAS O4 measurements: A new technique to derive information on atmospheric aerosols: 2. Modeling studies, J. Geophys. Res. 111, D14203, 10.1029/2005JD006618, 2006.

Garane, K., Bais, A. F., Kazadzis, S., Kazantzidis, A., and Meleti, C.: Monitoring of UV spectral irradiance at Thessaloniki (1990–2005): data re-evaluation and quality control, Ann. Geophys., 24, 3215–3228, https://doi.org/10.5194/angeo-24-3215-2006, 2006.

Garane, K., Fountoulakis, I., Karanikolas, A., Bais, A. F., and Meleti, C.: Thirty years of solar ultraviolet spectral irradiance measurements in Thessaloniki: Variability and trends, Radiation Processes In The Atmosphere And Ocean, AIP Conf. Proc. 18 January 2024, 2988, 090003, https://doi.org/10.1063/5.0183293, 2024.

Giles, D. M., Sinyuk, A., Sorokin, M. G., Schafer, J. S., Smirnov, A., Slutsker, I., Eck, T. F., Holben, B. N., Lewis, J. R., Campbell, J. R., Welton, E. J., Korkin, S. V., and Lyapustin, A. I.: Advancements in the Aerosol Robotic Network (AERONET) Version 3 database – automated near-real-time quality control algorithm with improved cloud screening for Sun photometer aerosol optical depth (AOD) measurements, Atmos. Meas. Tech., 12, 169–209, https://doi.org/10.5194/amt-12-169-2019, 2019.

Gröbner, J., Vergaz, R., Cachorro, V. E., Henriques, D. V., Lamb, K., Redondas, A., Vilaplana, J. M., and Rembges, D.: Intercomparison of aerosol optical depth measurements in the UVB using Brewer spectrophotometers and a Li-Cor spectrophotometer, Geophys. Res. Lett., 28, 1691–1694, https://doi.org/10.1029/2000GL012759, 2001.

Gröbner, J. and Meleti, C.: Aerosol optical depth in the UVB and visible wavelength range from Brewer spectrophotometer direct irradiance measurements: 1991–2002, J. Geophys. Res., 109, D09202, https://doi.org/10.1029/2003JD004409, 2004.

Gröbner, J., Kouremeti, N., Hülsen, G., Zuber, R., Ribnitzky, M., Nevas, S., Sperfeld, P., Schwind, K., Schneider, P., Kazadzis, S., Barreto, Á., Gardiner, T., Mottungan, K.,

Medland, D., and Coleman, M.: Spectral aerosol optical depth from SI-traceable spectral solar irradiance measurements, Atmos. Meas. Tech., 16, 4667–4680, https://doi.org/10.5194/amt-16-4667-2023, 2023.

Gröbner, J. and Kouremeti, N.: The Precision solar Spectroradiometer (PSR) for direct solar irradiance measurements, Sol. Energy, 185, 199–210, 10.1016/j.solener.2019.04.060, 2019.

Gröbner, J., Kouremeti, N., & Herreras, M.: Evaluation of Aeronet AOD at 1640 nm in scenarios with collocated instruments, Zenodo, https://doi.org/10.5281/zenodo.14639659, 2024.

Hönninger, G., von Friedeburg, C., and Platt, U.: Multi axis differential optical absorption spectroscopy (MAX-DOAS), Atmos. Chem. Phys., 4, 231–254, https://doi.org/10.5194/acp-4-231-2004, 2004.

Hrabčák, P.: Comparison of the optical depth of total ozone and atmospheric aerosols in Poprad-Gánovce, Slovakia, Atmos. Chem. Phys., 18, 7739–7755, https://doi.org/10.5194/acp-18-7739-2018, 2018.

Hrabčák, P., Garcia-Suñer, M., Matos, V., Estellés, V., Pribullová, A., Depta, J., Staněk, M., and Stráník, M.: 30 years of total column ozone and aerosol optical depth measurements using the Brewer spectrophotometer in Poprad-Gánovce, Slovakia, Atmos. Chem. Phys., 25, 16263–16286, https://doi.org/10.5194/acp-25-16263-2025, 2025.

Jaroslawski, J., Krzyścin, J. W., Puchalski, S., and Sobolewski, P.: On the optical thickness in the UV range: Analysis of the ground-based data taken at Belsk, Poland, J. Geophys. Res., 108, 4800, 0.1029/2003JD003571, 2003.

Ji, D., Sun, X., Ritter, C., and Notholt, J.: Retrieval of aerosol composition from spectral aerosol optical depth and optical properties using a machine learning approach, Atmos. Meas. Tech., 19, 421–436, https://doi.org/10.5194/amt-19-421-2026, 2026.

Karagkiozidis, D., Friedrich, M. M., Beirle, S., Bais, A., Hendrick, F., Voudouri, K. A., Fountoulakis, I., Karanikolas, A., Tzoumaka, P., Van Roozendael, M., Balis, D., and Wagner, T.: Retrieval of tropospheric aerosol, NO2, and HCHO vertical profiles from MAX-DOAS observations over Thessaloniki, Greece: intercomparison and validation

of two inversion algorithms, Atmos. Meas. Tech., 15, 1269–1301, https://doi.org/10.5194/amt-15-1269-2022, 2022.

Karanikolas, A., Torres, B., Momoi, M., Herreras-Giralda, M., Kouremeti, N., Gröbner, J., Doppler, L., and Kazadzis, S.: Retrieval of Aerosol Properties from Direct Solar Irradiance Measurements with High Temporal Resolution and Spectral Range, Atmos. Meas. Tech., 18, 7651–7677, https://doi.org/10.5194/amt-18-7651-2025, 2025.

Karanikolas, A.: Advancements in ground-based aerosol optical depth measurement and measurement-modelling synergies, ETH Zurich Research Collection, DISS. No. 32143, https://doi.org/10.3929/ethz-c-000806830, 2026.

Karsten, F. and Young, A. T.: Revised optical air mass tables and approximation formula, Appl. Opt., 28, 4735–4738, https://doi.org/10.1364/AO.28.004735, 1989.

Kasten, F.: A new table and approximation formula for the relative optical air mass, Arch. Meteorol. Geophys. Bioklimatol. Ser. B, 14, 206–223, https://doi.org/10.1007/BF02248840, 1966.

Kazadzis, S., Bais, A., Amiridis, V., Balis, D., Meleti, C., Kouremeti, N., Zerefos, C. S., Rapsomanikis, S., Petrakakis, M., Kelesis, A., Tzoumaka, P., and Kelektsoglou, K.: Nine years of UV aerosol optical depth measurements at Thessaloniki, Greece, Atmos. Chem. Phys., 7, 2091–2101, https://doi.org/10.5194/acp-7-2091-2007, 2007.

Kazadzis, S., Bais, A., Kouremeti, N., Gerasopoulos, E., Garane, K., Blumthaler, M., Schallhart, B. and Cede, A.: Direct spectral measurements with a Brewer spectroradiometer: absolute calibration and aerosol optical depth retrieval. Applied optics, 44(9), pp.1681-1690, https://doi.org/10.1364/AO.44.001681, 2005.

Kazadzis, S., Estellés, V., G. Campanelli, M. and Scarlatti F.: Report on the links of metrology MAPP project results and measurement accuracy and uncertainty improvements and an example of machine learning techniques towards the retrieval of aerosol properties , COST ACTION, COST-EUROPEAN COOPERATION IN SCIENCE AND TECHNOLOGY, Brussels, Belgium, https://harmonia-cost.eu/wp-content/uploads/2024/11/Harmonia_D23_f.pdf (last access: 16 October 2026), 2024.

Kazadzis, S., Kouremeti, N., and Gröbner, J.: Fifth WMO Filter Radiometer Comparison (FRC-V) 27 September to 25 October 2021, Davos, Switzerland, WMO

GAW report 280, https://library.wmo.int/records/item/66263-fifth-wmo-filter-radiometer-comparison-frc-v?offset=5 (last access: 1 February 2024), 2023.

Kazadzis, S., Kouremeti, N., Diémoz, H., Gröbner, J., Forgan, B. W., Campanelli, M., Estellés, V., Lantz, K., Michalsky, J., Carlund, T., Cuevas, E., Toledano, C., Becker, R., Nyeki, S., Kosmopoulos, P. G., Tatsiankou, V., Vuilleumier, L., Denn, F. M., Ohkawara, N., Ijima, O., Goloub, P., Raptis, P. I., Milner, M., Behrens, K., Barreto, A., Martucci, G., Hall, E., Wendell, J., Fabbri, B. E., and Wehrli, C.: Results from the Fourth WMO Filter Radiometer Comparison for aerosol optical depth measurements, Atmos. Chem. Phys., 18, 3185–3201, https://doi.org/10.5194/acp-18-3185-2018, 2018.

Kerr, J., McElroy, C., Wardle, D., Olafson, R., and Evans, W.: The Automated Brewer spectrophotometer, in: Atmospheric Ozone, edited by: Zerefos, C. and Ghazi, A., 396–401, Springer Netherlands, 10.1007/978-94-009-5313-0, 1985.

Komhyr, W. D., Harris, T. B., Waterman, L. S., Chin, J. F. S., and Thoning, K. W.: Atmospheric carbon dioxide at Mauna Loa Observatory: 1. NOAA global monitoring for climatic change measurements with a nondispersive infrared analyzer, 1974–1985, J. Geophys. Res., 94, 8533–8547, https://doi.org/10.1029/JD094iD06p08533, 1989.

Komhyr, W. D. and Evans, R. D.: Operations Handbook – Ozone Observations with a Dobson Spectrophotometer, rev. ed., GAW Report No. 183, World Meteorological Organization, Geneva, Switzerland, https://gml.noaa.gov/ozwv/dobson/GAW183-Dobson-WEB.pdf, 2008.

Kouremeti, N., Nevas, S., Kazadzis, S., Groebner, J., Schneider, P., and Schwind, K. M.: SI-traceable solar irradiance measurements for aerosol optical depth retrieval, Metrologia, 59, 044001, https://doi.org/10.1088/1681-7575/ac747d, 2022.

Kumharn, W., Rimmer, J. S., Smedley, A. R. D., Ying, T. Y., and Webb, A. R.: Aerosol optical depth and the Global Brewer Network: a study using U.K.- and Malaysia-based Brewer spectrophotometers, J. Atmos. Ocean. Tech., 29, 857–866, https://doi.org/10.1175/JTECH-D-11-00029.1, 2012.

Kumharn, W., Sudhibrabha, S., and Hanprasert, K.: Aerosol optical depth: a study using Thailand based Brewer spectrophotometers, Adv. Space Res., 56, 2384–2388, https://doi.org/10.1016/j.asr.2015.09.031, 2015.

Kudo, R., Diémoz, H., Estellés, V., Campanelli, M., Momoi, M., Marenco, F., Ryder, C. L., Ijima, O., Uchiyama, A., Nakashima, K., Yamazaki, A., Nagasawa, R., Ohkawara, N., and Ishida, H.: Optimal use of the Prede POM sky radiometer for aerosol, water vapor, and ozone retrievals, Atmos. Meas. Tech., 14, 3395–3426, https://doi.org/10.5194/amt-14-3395-2021, 2021.

Liu, O., Li, Z., Lin, Y., Fan, C., Zhang, Y., Li, K., Zhang, P., Wei, Y., Chen, T., Dong, J., and de Leeuw, G.: Evaluation of the first year of Pandora NO2 measurements over Beijing and application to satellite validation, Atmos. Meas. Tech., 17, 377–395, https://doi.org/10.5194/amt-17-377-2024, 2024.

López-Solano, J., Redondas, A., Carlund, T., Rodriguez-Franco, J. J., Diémoz, H., León-Luis, S. F., Hernández-Cruz, B., Guirado-Fuentes, C., Kouremeti, N., Gröbner, J., Kazadzis, S., Carreño, V., Berjón, A., Santana-Díaz, D., Rodríguez-Valido, M., De Bock, V., Moreta, J. R., Rimmer, J., Smedley, A. R. D., Boulkelia, L., Jepsen, N., Eriksen, P., Bais, A. F., Shirotov, V., Vilaplana, J. M., Wilson, K. M., and Karppinen, T.: Aerosol optical depth in the European Brewer Network, Atmos. Chem. Phys., 18, 3885–3902, https://doi.org/10.5194/acp-18-3885-2018, 2018.

Marenco, F., Di Sarra, A., and De Luisi, J.: Methodology for determining aerosol optical depth from Brewer 300–320 nm ozone measurements, Appl. Opt., 41, 1805–1814, https://doi.org/10.1364/AO.41.001805, 2002.

Masoom, A., Kazadzis, S., Valeri, M., Raptis, I.-P., Brizzi, G., Papachristopoulou, K., Barnaba, F., Casadio, S., Kreuter, A., and Niro, F.: Assessment of the impact of NO2 contribution on aerosol-optical-depth measurements at several sites worldwide, Atmos. Meas. Tech., 17, 5525–5549, https://doi.org/10.5194/amt-17-5525-2024, 2024.

Masoom, A., Kazadzis, S., Modini, R. L., Gysel-Beer, M., Gröbner, J., Coen, M. C., Navas-Guzman, F., Kouremeti, N., Brem, B. T., Nowak, N. K., Martucci, G., Hervo, M., and Erb, S.: Long range transport of Canadian wildfire smoke to Europe in 2023: aerosol properties and spectral features of smoke particles, Atmos. Chem. Phys., 26, 10801–10834, https://doi.org/10.5194/acp-26-10801-2026, 2026.

Molina, M. J. and Rowland, F. S.: Stratospheric sink for chlorofluoromethanes: chlorine atom-catalysed destruction of ozone, Nature, 249 (5460), 810–812, https://doi.org/10.1038/249810a0, 1974.

Pathakoti, M., Mahalakshmi, D. V., Kanchana, A. L., Rajan, K. S., Taori, A., Bothale, R. V., and Chauhan, P.: Temporal variability of atmospheric columnar CO2, CH4, CO and N2O concentrations using ground-based remote sensing FTIR Spectrometer, Adv. Space Res., 73, 4967–4975, https://doi.org/10.1016/j.asr.2024.02.028, 2024.

Pribullová, A.: Spectral UV aerosol optical thickness determinated from the Poprad-Gánovce Brewer spectrophotometer observations, Contrib. Geophys. Geodesy., 32, 291–307, 2002.

Redondas, A., Evans, R., Stuebi, R., Köhler, U., and Weber, M.: Evaluation of the use of five laboratory-determined ozone absorption cross sections in Brewer and Dobson retrieval algorithms, Atmos. Chem. Phys., 14, 1635–1648, https://doi.org/10.5194/acp-14-1635-2014, 2014.

Richard, E., Harber, D., Coddington, O., Drake, G., Rutkowski, J., Triplett, M., Pilewskie, P., and Woods, T.: SI-traceable spectral irradiance radiometric characterization and absolute calibration of the TSIS-1 Spectral Irradiance Monitor (SIM), Remote Sens.-Basel, 12, 1818, https://doi.org/10.3390/rs12111818, 2020.

Ritter, C., Notholt, J., Fisher, J., and Rathke, C.: Direct thermal radiative forcing of tropospheric aerosol in the Arctic measured by ground based infrared spectrometry, Geophys. Res. Lett., 32, L23816, 10.1029/2005GL024331, 2005.

SCI-TEC Instruments Inc.: Brewer MKIV Spectrophotometer Operator's Manual. Technical Report OM-BA-C231 REV B, Saskatoon, Saskatchewan, Canada, https://www.esrl.noaa.gov/gmd/grad/neubrew/docs/manuals/Brewer_Operator_wTOC.pdf?utm_source=chatgpt.com, 1999.

Seo, J., Choi, H., and Oh, Y.: Potential of AOD retrieval using atmospheric emitted radiance interferometer (AERI), Remote Sens., 14, 407, https://doi.org/10.3390/rs14020407, 2022.

Thomas, M., Gautier, C., and Ricchiazzi, P.: Investigations of the March 2006 African dust storm using ground-based column-integrated high spectral resolution infrared

(8–13 μm) and visible aerosol optical thickness measurements: 1. Measurement procedures and results, J. Geophys. Res., 114, D11202, 10.1029/2008JD010928, 2009.

Shaw, G. E., Reagan, J. A., and Herman, B. M.: Investigations of Atmospheric Extinction Using Direct Solar Radiation Measurements Made with a Multiple Wavelength Radiometer, J. Appl. Meteorol. Clim., 12, 374–380, https://doi.org/10.1175/1520-0450(1973)012<0374:IOAEUD>2.0.CO;2, 1973.

Staehelin, J., Viatte, P., Stübi, R., Tummon, F., and Peter, T.: Stratospheric ozone measurements at Arosa (Switzerland): history and scientific relevance, Atmos. Chem. Phys., 18, 6567–6584, https://doi.org/10.5194/acp-18-6567-2018, 2018.

Wagner, T., Dix, B., Friedeburg, v. C., Friess, U., Sanghavi, S., Sinreich, R., and Platt, U.: MAX-DOAS O4 measurements: A new technique to derive information on atmospheric aerosols Principles and information content, J. Geophys. Res., 109, D22205, 10.1029/2004JD004904, 2004.

Wang, Z., Liu, D., Wang, Z., Wang, Y., Khatri, P., Zhou, J., Takamura, T., and Shi, G.: Seasonal characteristics of aerosol optical properties at the SKYNET Hefei site (31.90◦ N, 117.17◦ E) from 2007 to 2013, J. Geophys. Res. Atmos., 119, 6128–6139, doi:10.1002/2014JD021500, 2014.

WMO: Aerosol measurement procedures, guidelines and recommendations, GAW Report 153, WMO/TD-No 1178, https://gml.noaa.gov/aero/docsGAW_153_Aerosol_Measurement_Procedures.pdf (last access: 12 December 2025), 2003.

WMO (World Meteorological Organization), Scientific Assessment of Ozone Depletion: 2022, Ozone research and monitoring - GAW report No. 278, Geneva, Switzerland, https://library.wmo.int/idurl/4/58360, 2022.

Zuber, R., Sperfeld, P., Riechelmann, S., Nevas, S., Sildoja, M., and Seckmeyer, G.: Adaption of an array spectroradiometer for total ozone column retrieval using direct solar irradiance measurements in the UV spectral range, Atmos. Meas. Tech., 11, 2477–2484, https://doi.org/10.5194/amt-11-2477-2018, 2018.

List of figures

3.1: Aerial view of the Poprad-Gánovce station and the Brewer ozone spectrophotometer on the station's roof.

3.2: The long-term monthly characteristics of AOD at 320 nm for Poprad-Gánovce obtained over the 32-year period (1994–2025).

3.3: Comparison of annual mean AOD at the two longest Brewer wavelengths and their linear trends in Poprad-Gánovce over the 32-year period (1994–2025).

4.1: BTS spectroradiometers in PMOD/WRC, Davos.

4.2: Statistics of AOD differences between observed and predicted AOD from 17637 BTS observations in the 2023–2025 period for different wavelength selections.

4.3: Example of AOD retrievals from BTS in Davos on 28/10/2024 at 12.85 UTC.

4.4: Example of AOD retrievals from BTS in Davos on 19/6/2024 at 9:10 UTC, during transport of Saharan dust to the Alps.

4.5: Example of AOD retrievals from BTS in Davos on 1/10/2023 at 10:00 UTC, during transport of smoke from Canadian wildfires to Europe.

Appendix

Table A1: Acronyms.

AE	Ångström Exponent
AERI	Atmospheric Emitted Radiance Interferometer
AERONET	AErosol RObotic NETwork
AOD	Aerosol Optical Depth (also known as AOT: Aerosol Optical Thickness)
BTS	BiTec Sensor (type of array spectroradiometer)
CH_4	Methane
CO	Carbon Monoxide
CO_2	Carbon Dioxide
DNA	DeoxyriboNucleic Acid
DU	Dobson Unit
DWD	Deutscher Wetterdienst (German meteorological service)
EUBREWNET	European Brewer Network
FTIR	Fourier-Transform Infrared Spectroscopy
GAW-PFR	Global Atmosphere Watch - Precision Filter Radiometer
GRASP	Generalised Retrieval of Atmosphere and Surface Properties
HARMONIA	International network for harmonisation of atmospheric aerosol retrievals from ground-based photometers: Name of the COST action
H_2O	Water Vapour
IOS	International Ozone Services
IR	Infrared
MAX-DOAS	Multi AXis Differential Optical Absorption Spectroscopy
MFR-SR	Multifilter Rotating Shadowband Radiometer
N_2O	Nitrous Oxide

NO_2	Nitrogen Dioxide
NOAA	National Oceanic and Atmospheric Administration
O_3	Ozone
O_4	Collision-induced interactions between two oxygen molecules (molecular oxygen dimers)
PFR	Precision Filter Radiometer
PSR	Precision Spectroradiometer
PMOD/WRC	Physikalisch-Meteorologisches Observatorium Davos and World Radiation Center
POM	Prede-POM sun and sky radiometer
PTB	Physikalisch-Technische Bundesanstalt
R	Pearson correlation coefficient
R^2	Pearson coefficient of determination
RMSE	Root Mean Square Error
SO_2	Sulphur Dioxide
SI	International System of Units
SSA	Single Scattering Albedo
STSM	Short Term Scientific Mission
SZA	Solar Zenith Angle
UV	Ultraviolet
VM	Virtual Mobility
WG	Working Group
WMO	World Meteorological Organisation

Acknowledgements

Angelos Karanikolas would like to thank Dr. Julian Gröbner for the retrievals of the BTS optical depth and Mr. Dhrona Jaine Kochuparambil for the retrieval of BTS water vapour necessary to correct the optical depths in the infrared.